

NJC

Accepted Manuscript



This is an *Accepted Manuscript*, which has been through the Royal Society of Chemistry peer review process and has been accepted for publication.

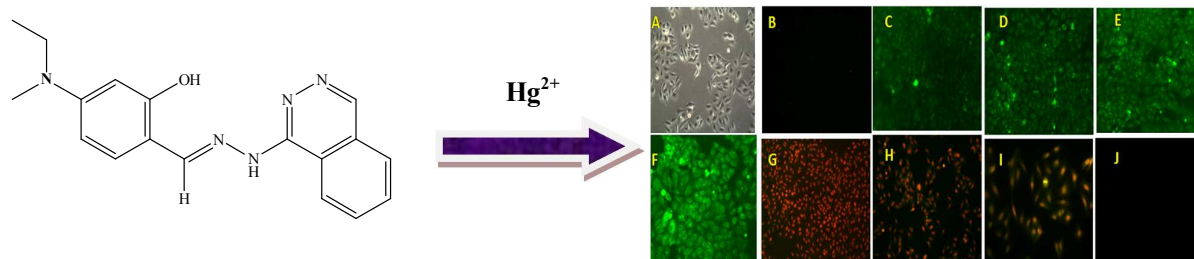
Accepted Manuscripts are published online shortly after acceptance, before technical editing, formatting and proof reading. Using this free service, authors can make their results available to the community, in citable form, before we publish the edited article. We will replace this *Accepted Manuscript* with the edited and formatted *Advance Article* as soon as it is available.

You can find more information about *Accepted Manuscripts* in the [Information for Authors](#).

Please note that technical editing may introduce minor changes to the text and/or graphics, which may alter content. The journal's standard [Terms & Conditions](#) and the [Ethical guidelines](#) still apply. In no event shall the Royal Society of Chemistry be held responsible for any errors or omissions in this *Accepted Manuscript* or any consequences arising from the use of any information it contains.



www.rsc.org/njc



Graphical Abstract

Sensor **1** showed a high selectivity and sensitivity towards Hg^{2+} by giving significant fluorescent enhancement.

A highly selective fluorescent ‘turn-on’ chemosensor for Hg²⁺ based on a phthalazin-hydrazone derivative and its application in human cervical cancer cells imaging

Dipesh Mahajan^a, Nilesh Khairnar^a, Banashree Bondhopadhyay^c, Suban K.Sahoo^b, Anupam

Basu^c, Jasminder Singh^d, Narinder Singh^{*d}, Ratnamala Bendre^{*a}, Anil Kuwar^{*a}

^aSchool of Chemical Sciences, North Maharashtra University, Jalgaon (MS), India.

^bDepartment of Chemistry, SV National Institute Technology, Surat (Gujarat), India.

^cMolecular Biology and Human Genetics Laboratory, Department of Zoology, The University of Burdwan, Burdwan (West Bengal), India.

^dDepartment of Chemistry, Indian Institute Technology, Ropar (Punjab), India.

Abstract

A new phthalazin-hydrazone based fluorescent chemosensor (E)-5-(diethylamino)-2-((2-(phthalazin-1-yl)hydrazono)methyl)phenol (**1**) was reported. Sensor **1** showed a high selectivity and sensitivity towards Hg²⁺ by giving significant fluorescent enhancement at 550 nm over other tested cations in DMSO/H₂O (80:20, v/v) medium. The association constant of $1.0 \times 10^4 \text{ M}^{-1}$ between the sensor **1** and Hg²⁺. Sensor **1** showed a nanomolar detection limit of 26.1 nM Hg²⁺. Finally, the fluorescence imaging experiments for the detection of intracellular Hg²⁺ in human cervical cancer HeLa cells showed its practical utility in biological samples.

Keywords: Fluorescent ‘turn-on’ sensor, Hg²⁺, live cells imaging, DFT.

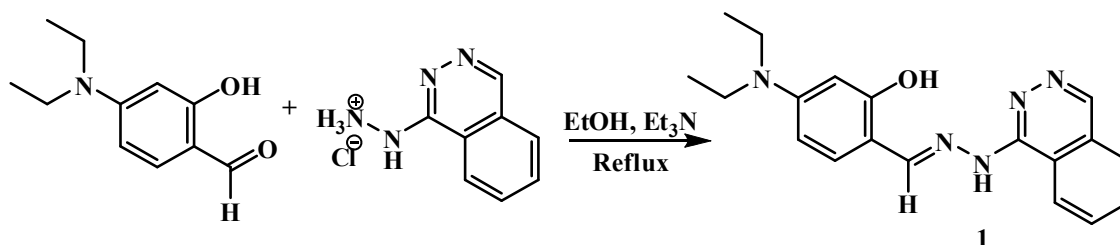
*Corresponding authors E-mail: kuwaras@gmail.com, bendreras@rediffmail.com, nsingh@iitrpr.ac.in

Introduction

The design and applications of fluorescent chemosensors for the qualitative and quantitative monitoring of bioactive cations and anions have gained an immense significance in the current research and innovation, because of their simplicity and quick finding of target analytes in different biological, environmental and industrial samples [1-4]. The fluorescence of chemosensors may be quenched, enhanced or ratiometrically shifted upon selective interaction with the target analyte due to energy/electron/charge transfer facilitates the quick detection. Among all cations and anions, Hg^{2+} is one of the most detrimental and widespread heavy metal ions distributed in the eco-system [5]. The international regulatory agencies, like, environmental protection agency (EPA) have set an upper limit of 2 ppb (10 nM) for Hg^{2+} to avoid toxicity in drinking water. The detrimental Hg^{2+} ions is easily converted into organomercury species (like methylmercury) *via* a biotic or abiotic path, and accumulates in human body by entering through the food chain which causes a wide variety of health problems including digestive, kidney, neurological and Minamata diseases [6-8]. Therefore, great quantities of fluorescent chemosensors for Hg^{2+} have been planned up to now in order to avoid the requirement of complicated and sophisticated instrumentation in the currently used analytical techniques such as atomic absorption, atomic emission and inductively coupled plasma spectroscopy [9-11]. However, the reported Hg^{2+} fluorescent chemosensors are mainly based on fluorescence ‘turn-off’ due to the well-known heavy metal quenching effects occurs via a number of pathways including spin-orbit coupling. As ‘turn-on’ fluorescent sensor is preferable over ‘turn-off’, there is an immense interest in the designing of easy-to-prepare ‘turn-on’ sensor to detect Hg^{2+} and other such metals from aqueous medium and also their applications in various biological samples [12].

In this article, we have developed a novel fluorescent chemosensor (E)-5-(diethylamino)-2-((2-(phthalazin-1-yl)hydrazono)methyl)phenol (receptor **1**) (**Scheme 1**) for

the detection of Hg^{2+} in DMSO/ H_2O (80:20, v/v) medium. This sensor showed an elevated sensitivity with 'turn-on' fluorescence reply towards Hg^{2+} ions and high-quality selectivity in the presence of other examinational cations. Further, the use of receptor **1** for the discovery of Hg^{2+} in living cells was examined using HeLa cancer cell lines, which exhibited a well-built fluorescence as monitored by confocal fluorescence microscopy.



Scheme 1. Synthesis of receptor **1**.

Experimental

All starting chemicals and reagents of analytical grade were obtained commercially from Sigma-Aldrich and Merck Chemical Ltd., and were used without further purification. NMR spectra were recorded at room temperature on a Varian 400 MHz spectrometer in DMSO-d_6 . Chemical shifts are expressed in δ units. IR spectra were obtained on a Perkin Elmer Spectrum 100 FTIR spectrometer. Fluorescence spectra were recorded with a Horiba fluorescence spectrofluorometer at room temperature. Absorption spectra were carried out on a Perkin Elmer spectrophotometer.

Synthesis of (E)-5-(diethylamino)-2-((2-(phthalazin-1-yl)hydrazono)methyl)phenol

To phthalazin hydrochloride (0.001 mol) in ethanol, triethylamine (0.0012 mol) was added and the solution was stirred for 5-10 min. Then, 4-(diethylamino)-2-hydroxybenzaldehyde (0.001 mol) was added in above solution. The mixture was heated with stirring for 3-4 hrs. The progress of reaction was monitored by TLC. After completion of reaction, the obtained precipitate was filtered and washed with small quantity of ethanol, so as to obtain pure product. Receptor **1** was obtained as a pale yellow precipitate. Yield: 85 %.

LC-MS:m/z, calcd for C₁₉H₂₁N₅O (M+H⁺) 336.17 found 336.1. ¹H- NMR (400MHz, DMSO-*d*₂): 1.08-1.13(t, 6H, 2CH₃), 3.29-3.42(quart, 4H, 2CH₂), 6.12(s, 1H, Ar-H), 6.24-6.27(d, 1H, Ar-H), 7.32-7.35(d, 1H, Ar-H), 7.65-7.70(m, 3H, Ar-H), 8.21-8.24(d, 1H, Ar-H), 8.46(s, 1H, Ar-H), 10.36(s, 1H, -OH), 11.83(s, 1H, NH). ¹³C- NMR (100MHz, DMSO-*d*₂): 12.20, 43.42, 96.83, 103.31, 107.37, 123.01, 126.10, 131.5, 136.87, 144.62, 149.63, 156.02, 158.84.

UV-visible and fluorescence spectral measurements

The metal ions Na⁺, K⁺, Ca²⁺, Mg²⁺, Al³⁺, Ba²⁺, Ce³⁺, Fe³⁺, Co²⁺, Ni²⁺, Cu²⁺, Zn²⁺, Hg²⁺, Pb²⁺, Cd²⁺, Th⁴⁺ and Ag⁺ were added as their nitrate salts where as Sr²⁺ and Mn²⁺ were added as their chloride salts for the different absorption and fluorescence spectroscopic experiments. Stock solutions of metal ions (1 × 10⁻³ M) and the sensor **1** (1 × 10⁻⁴ M) were prepared in DMSO/H₂O (80:20, v/v). These stock solutions were used for different spectroscopic experiments after appropriate dilution. For the absorbance and fluorescence measurements, 1 cm width and 3.5 cm height quartz cells were used. The excitation was carried out at 414 nm for sensor **1** with 5 nm emission slit widths in fluorometer.

In vitro cell imaging

To detect Hg²⁺ in the live cells, human cervical cancer cells HeLa were cultured in DMEM media supplemented with 10% FBS and 2% Penicillin-Streptomycin in a humidified incubator at 37°C and with 5% CO₂. After attaining 70-80% confluence in 60mm culture dish, the HeLa cells were trypsinized and seeded in 35 mm culture dish. After overnight incubation, the cells were washed with serum free media. The cells were treated with Hg²⁺ (1 μM, 2.5 μM, 5 μM and 10 μM) for 10 minutes and then the receptor **1** (0.225 μM) was added in the same media. For the specific detection of Hg²⁺ with the help of sensor **1** at cytoplasm, the cells were counter stained with propidium iodide for distinguish the nucleolus. The cells were then observed under blue filter (450-490 nm) in inverted fluorescence microscope

(Leica DMI6000B). The fluorescence images of cells were captured in 20X and 40X objectives through an attached CCD camera using acquisition software.

Results and discussion

The sensor **1** was synthesized by following our reported procedure [13]. As shown in **Scheme 1**, the sensor **1** was synthesized by reacting 4-(diethylamino)-2-hydroxybenzaldehyde with phthalazin hydrochloride in the presence of triethylamine for 3-4 hrs in ethanolic medium. The proposed molecular structure of **1** was characterized by $^1\text{H-NMR}$, $^{13}\text{C-NMR}$ and LC-MS (**Figure S1-3**, Supporting information).

The UV-visible spectroscopic performances of sensor **1** (1×10^{-4} M) were first investigated upon addition of different cations (1×10^{-3} M) such as Co^{2+} , Ni^{2+} , Cu^{2+} , Mg^{2+} , Zn^{2+} , Hg^{2+} , Zr^{2+} , Cs^+ , Cd^{2+} , Ca^{2+} , Ba^+ , Fe^{2+} , Fe^{3+} , Pb^{2+} , Mn^{2+} , K^+ , Al^{3+} , Sr^{2+} and Na^+ in DMSO/ H_2O (80:20, v/v). The sensor **1** (1×10^{-4} M) showed a strong peak at 414 nm with molar absorption coefficients of $8.83 \times 10^3 \text{ cm}^{-1} \text{ M}^{-1}$. The absorption peak at 414 nm of free sensor **1** was red shifted to 425 nm due to intramolecular charge transfer (ICT) effect upon addition of 1 equivalent Hg^{2+} (**Figure 1**). The red shift in the UV-Vis absorption spectra of **1** was also observed from the titration study (**Figure 2**), where the Hg^{2+} ions (0–5 equivalents) was added successively to a fixed concentration of **1** (1×10^{-4} M). The spectral changes clearly delineated the complexation reaction occurred between the sensor **1** and Hg^{2+} .

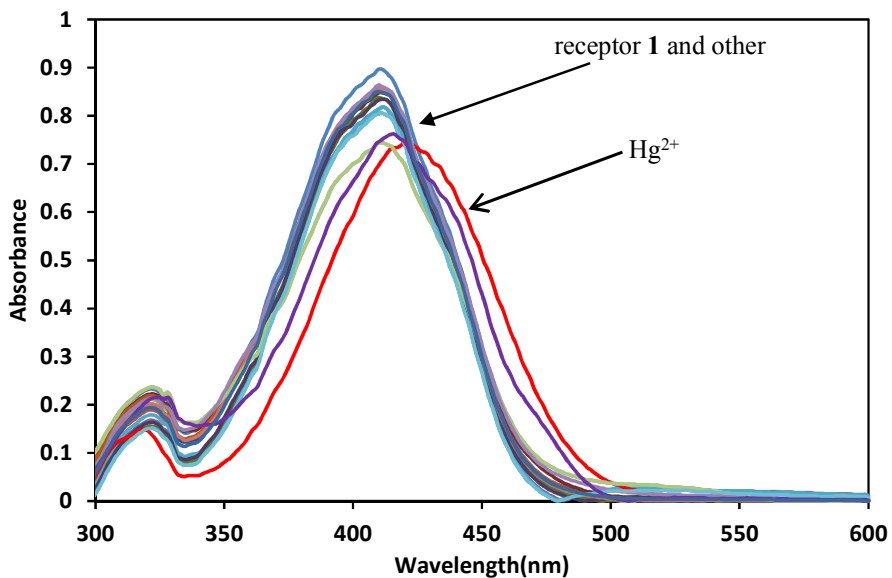


Figure 1. UV-Vis spectra changes of the sensor **1** (1×10^{-4} M) upon addition of various cations (1×10^{-3} M) in DMSO/H₂O (80:20, v/v).

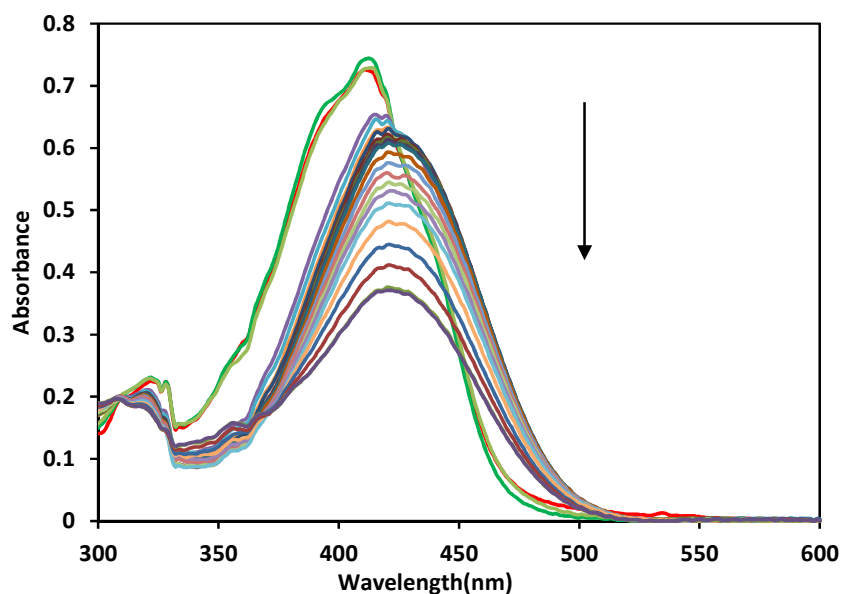


Figure 2. UV-Vis spectra titration of the sensor **1** (1×10^{-4} M) upon addition of various concentrations of Hg²⁺ (1×10^{-3} M) in DMSO/H₂O (80:20, v/v).

The cation recognition and sensing ability of sensor **1** (1×10^{-4} M) in DMSO/H₂O (80:20, v/v) was examined upon addition of various cations (Co²⁺, Ni²⁺, Cu²⁺, Mg²⁺, Zn²⁺, Hg²⁺, Zr²⁺, Cs⁺, Cd²⁺, Ca²⁺, Ba⁺, Fe²⁺, Fe³⁺, Pb²⁺, Mn²⁺, K⁺, Al³⁺, Sr²⁺, Na⁺) (1×10^{-3} M) by

fluorescence spectroscopy (**Figure 3** and **S4**). The free sensor **1** showed a weak emission spectra at 514 nm ($\lambda_{\text{exc}} = 414$ nm). The addition of an equivalent of Hg^{2+} to receptor **1** resulted in a red shifting along with a significant enhancement in the fluorescence intensity centred at 550 nm. No meaningful changes in the fluorescence of **1** were observed upon addition of other cations. This result indicates the Hg^{2+} -selective fluorescent ‘turn-on’ chemosensing ability of sensor **1**. The Hg^{2+} -selective fluorescent enhancement may be attributed to the formation of a rigid $\mathbf{1.Hg}^{2+}$ complex which inhibited the C=N isomerisation at the excited state causing the chelation-enhanced fluorescence (CHEF) effect. Alternately, the possible coordination of Hg^{2+} through the hydroxyl-O, imine-N and phthalazin-N atoms of sensor **1** blocked the photoinduced electron transfer (PET) process which causes a ‘turn-on’ emission.

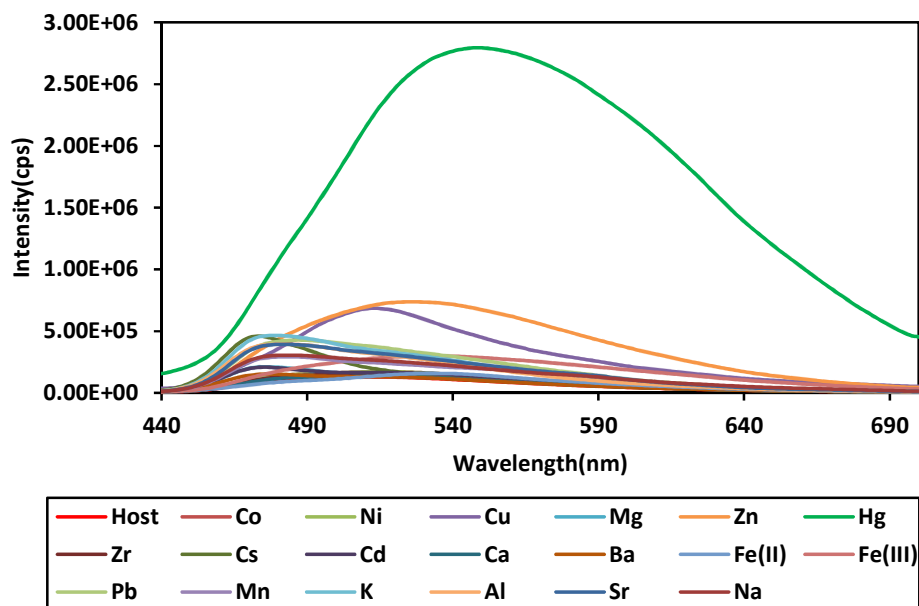


Figure 3. Changes in the emission sketch of the sensor **1** (1×10^{-4} M) upon addition of particular cations (1×10^{-3} M) in DMSO/ H_2O (80:20, v/v).

To get more fuller insight into the fluorosensing ability of Hg^{2+} by the sensor **1**, the fluorometric titration was performed by continuous addition of Hg^{2+} ions (0–800 μL) to a fixed concentration of sensor **1** solution (**Figure 4**). From the fluorescent titrations, the

association constant of $1.0 \times 10^4 \text{ M}^{-1}$ was calculated by Bensi-Hildbrand method for Hg^{2+} (**Figure S5**) [14]. In the DMSO/ H_2O (80:20, v/v) containing solvent system, the calculated detection limit for Hg^{2+} was 26.1 nM calculated using standard IUPAC method of 3σ method (Table S1), which is lower than many reported detection limits so far [15, 17-27]. Further, to get analytical application of sensing possessions of sensor **1** toward Hg^{2+} , the fluorescence emission of different competitive ions in DMSO/ H_2O (80:20, v/v) solution was examined, and the consequences were shown in **Figure 5**. No significant changes were observed when Cd^{2+} , Co^{2+} , Ni^{2+} , Cu^{2+} , Mg^{2+} , Zn^{2+} , Hg^{2+} , Zr^{2+} , Cs^+ , Cd^{2+} , Ca^{2+} , Ba^+ , Fe^{2+} , Fe^{3+} , Pb^{2+} , Mn^{2+} , K^+ , Al^{3+} , Sr^{2+} , Na^+ were added in the sensor **1** solution even at high concentration (10 equiv, red bars). Competition experimentations in the addition of Hg^{2+} (1 equiv) showed enhancement (yellow bars). This result clearly indicates the specificity of the sensor **1** to detect Hg^{2+} under competitive environment.

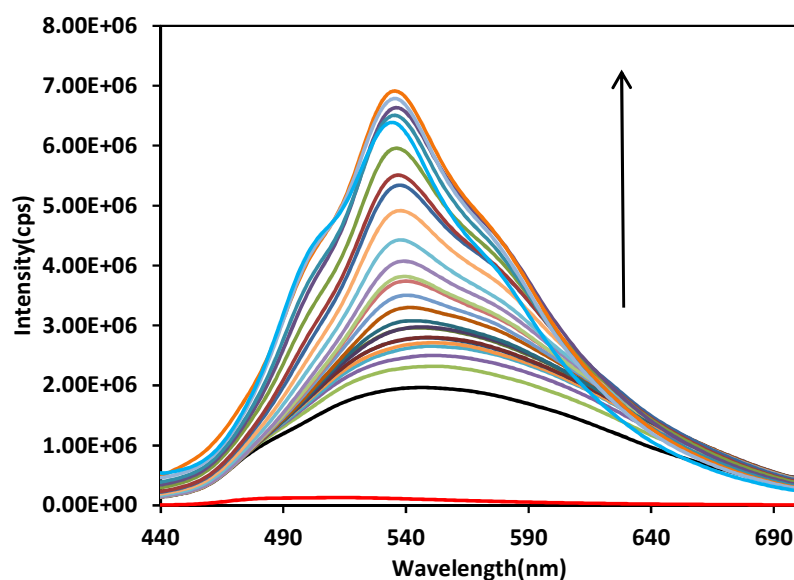


Figure 4. changes in the emission profile of the sensor **1** ($1 \times 10^{-4} \text{ M}$) upon successive addition of Hg^{2+} (0–800 μL) in DMSO/ H_2O (80:20, v/v).

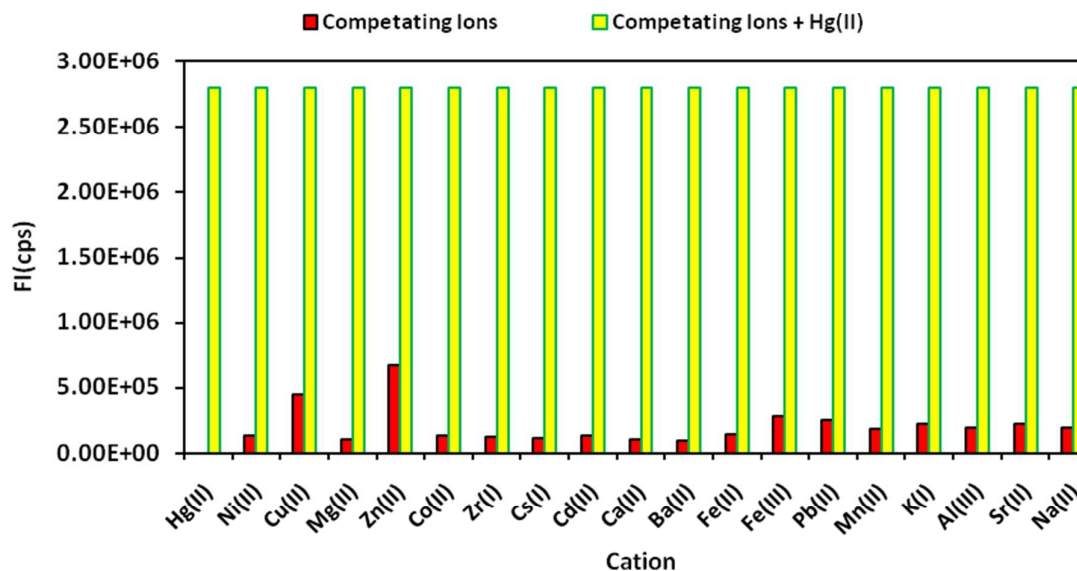


Figure 5. Fluorescence reply of sensor **1** (1 equivalent) to various cations (10 equivalents) in DMSO/H₂O solution (80:20, v/v). The yellow bars represent the fluorescent intensity of sensor **1** and Hg²⁺. The red bars represent the fluorescence changes that occur upon the addition of interference cations to the solution containing sensor **1** and Hg²⁺.

To study the workability of the proposed sensor and its sensitivity towards attaching with Hg²⁺ ions was tested by using various concentration of mercury ion and plotting its relative fluorescence with respect to time (**Figure S6**). It was quite evident from the plot that the reaction reaches a plateau at 30 seconds and remains stable afterwards, no matter what the concentration of mercury ions employed for the study.

To support the binding of Hg²⁺ with sensor **1**, NMR studies were carried out. It is quite evident from the study that, as the amount of mercury is increased in the sensor **1**. The characteristic peaks of the receptor get broadened due to attachment of mercury to the sensor **1**, causing the transfer of electrons from the nitrogen and oxygen atoms present in the receptor. The transfer of the electrons from the receptor to mercury ion itself causes increase in their electron withdrawing capacity of such atoms, leading to shift in the signal to the downfield region (**Figure 6**).

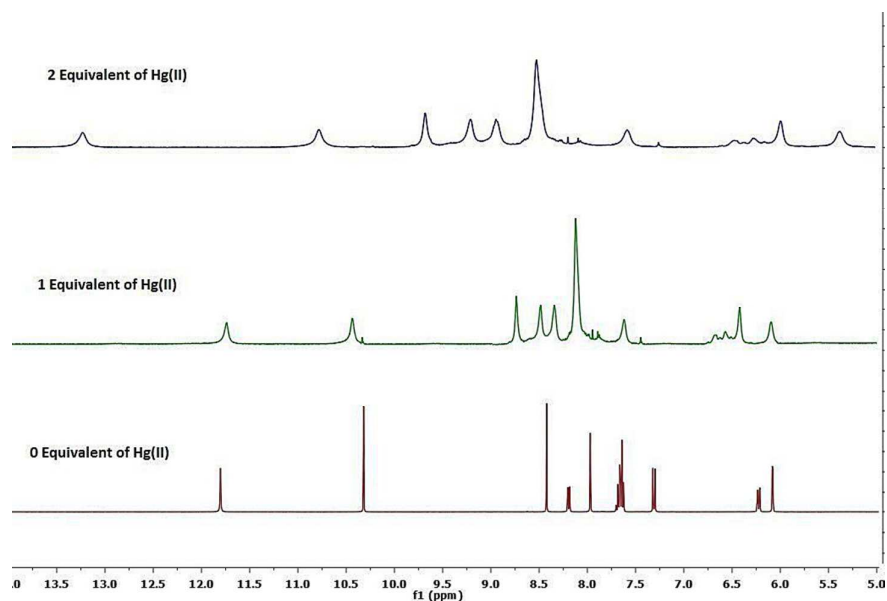


Figure 6: ^1H NMR titration of Receptor **1** with Hg^{2+} at different concentrations in DMSO-d_6 .

Further, the computational study was conducted by using the density functional theory (DFT) method to propose the possible 3D structure of sensor **1** and its complex with Hg^{2+} . The exchange-correlation function B3LYP with basis sets 6-31G** (for O, C, N, H atoms) and LanL2DZ (only for Hg^{2+}) was employed for the structural optimization in the gas phase by using the Gaussian 09W computational program [16]. The optimized structure of sensor **1** energetically preferred a planar enol-imine form where the possible donor atoms are present in the same side for easy encapsulation of Hg^{2+} ions (**Figure 7**). Upon complexation with Hg^{2+} , the calculated interaction energy ($E_{\text{int}} = E_{\text{complex}} - E_{\text{receptor}} - E_{\text{Hg}^{2+}}$) of -76.21 kcal/mol indicates the formation of a stable complex between **1** and Hg^{2+} . Also, there is an increase in the stability of the whole system. The band gap between HOMO-LUMO of sensor **1** alone becomes lowered for **1**. Hg^{2+} complex due to the possible charge transfer process occurred between the sensor **1** and Hg^{2+} ions (**Figure 7**).

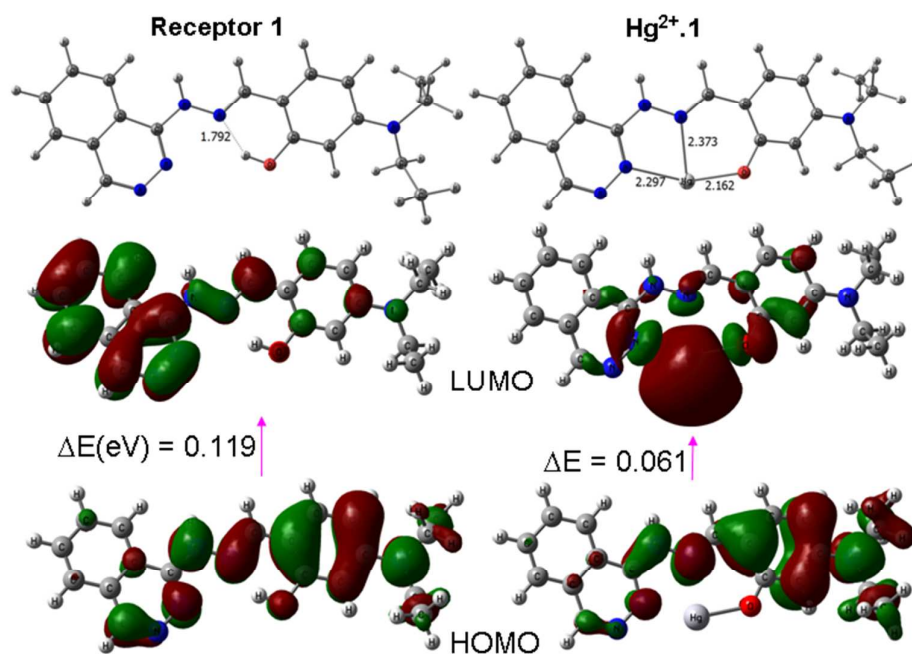


Figure 7. DFT computed optimized structure, HOMO, LUMO and the band gap of sensor **1** and **1-Hg²⁺**.

In live cells imaging study, it was observed that the sensor **1** interacts with cytoplasmic Hg^{2+} and produce a green fluorescence (**Figure 8**). The cells when treated with Hg^{2+} (1 μM , 2.5 μM , 5 μM and 10 μM) and sensor **1** (0.225 μM), and showed a gradual enhancement in the fluorescence intensity with the increase dose of Hg^{2+} . The counter staining with propidium iodide showed a clear red fluorescence at nucleolus. The cells when treated with Hg^{2+} (10 μM) or sensor **1** alone, showed no fluorescence from the cells (**Figure 8**). It is reported that Hg^{2+} can impair function of mitochondria, peroxisomes, etc which are situated in the cytoplasm of the cell. Impairing the power house of a cell means disrupting the oxygen supply. It is known that a cancer cell mainly thrives on the hypoxic condition. Thus, mercury probably helps the cancer cells to flourish. So, sensor **1** is the novel molecule which can detect specifically the cytoplasmic concentration of Hg^{2+} in cancer cells. The sensor **1** is biocompatible in nature and has an ability to get internalized in the cells very rapidly. Thus

best of our knowledge, no sensors are available, which can sense the cytoplasmic Hg^{2+} in the cancer cells and has huge potential application for diagnostic area.

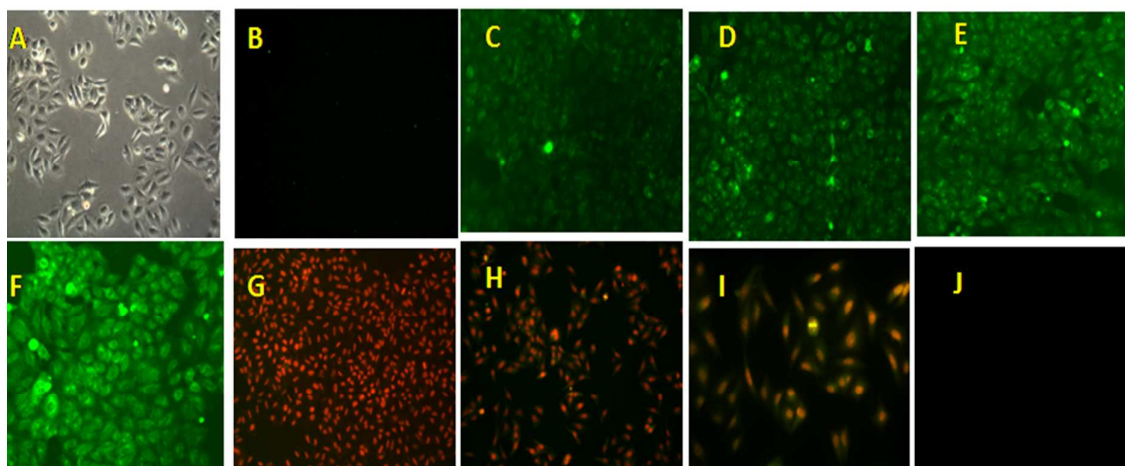


Figure 8. A) Phase contrast image of the control cells (20X), B) Fluorescent image of the cells treated with sensor **1** (0.225 μM) alone (20X), C) Fluorescent image of the cells treated with both Hg^{2+} (1.0 μM) and sensor **1** (0.25 μM) showing green fluorescence at cytoplasmic area only (20X), D) Fluorescent image of the cells treated with both Hg^{2+} (2.5 μM) and sensor **1** (0.25 μM) (20X), E) Fluorescent image of the cells treated with both Hg^{2+} (5.0 μM) and sensor **1** (0.25 μM) (20X), F) Fluorescent image of the cells treated with both Hg^{2+} (10 μM) and sensor **1** (0.25 μM) (40X), G) Fluorescent image of the cells treated with PI alone showing nucleolus only (20X), H) Fluorescent image of the cells treated with both Hg^{2+} (5 μM) and sensor **1** (0.25 μM) and counter stained with PI (20X), I) Fluorescent image of the cells treated with both Hg^{2+} (5 μM) and sensor **1** (0.25 μM) and counter stained with PI (40X), J) Fluorescent image of the cells treated with Hg^{2+} (10.0 μM) alone. All the fluorescent images were taken under Blue filter (450-490nm).

The prepared receptor has been compared with the recently reported sensors for mercury and their application in living cell imaging. It is quite evident from the table **1** that reported sensor is having quite an edge in respect of detection limit and its usage in real living cell imaging for detection of mercury in them.

Table 1: Comparison of reported sensors for mercury and their application in living cell imaging for determination of Hg^{2+} ions in them and with presented sensor **1**.

S. No	Reference	Solvent System	Detection Limit	Biological Application
1	Dalton Trans., 2013, 42, 4456 ¹⁷	CH_3CN	50 mM	No
2	Org. Lett., 2010, 12, 476 ¹⁸	$\text{C}_2\text{H}_5\text{OH}/\text{H}_2\text{O}(1:1; \text{v/v})$	80 μM	No
3	Org. Biomol. Chem., 2011, 9, 2350 ¹⁹	Water	5 mM	No
4	Analyst, 2012, 137, 3717 ²⁰	Water	260 nM	No
5	J. Mater. Chem. C, 2014, 2, 2534 ²¹	CH_3CN -PBS (7 : 3; v/v, pH 7.4)	-	No
6	Org. Biomol. Chem., 2010, 8, 3220 ²²	Water	10 pM	No
7	Spectrochim. Acta, Part A, 2012, 93, 245 ²³	DMSO	5.0 mM	No
8	Tetrahedron Lett., 2010, 51, 3286 ²⁴	CH_3CN -DDW	30 mM	No
9	Org. Biomol. Chem., 2012, 10, 5410 ²⁵	H_2O - CH_3CN (10:90, v/v)	0.226 mM	Yes
10	RSC Adv., 2012, 2, 10605 ²⁶	H_2O - CH_3CN (30:70, v/v)	22 nM	Yes
11	Spectrochimica Acta Part A: 2014, 123, 18 ²⁷	DMSO/ H_2O (9:1, v/v)	350 nM	No
12	Proposed System	DMSO/ H_2O (8:2, v/v)	26.1 nM	Yes

In conclusion, we have developed a novel fluorescent ‘turn-on’ chemosensor **1** based on a Schiff base derived from phthalazin hydrochloride and 4-(diethylamino)-2-hydroxybenzaldehyde. The sensor **1** exhibited a high selectivity and sensitivity for the detection of Hg^{2+} through significant fluorescence enhancement at 550 nm with a nonomolar detection limit. The sensor **1** can be utilized for the detection of Hg^{2+} in the presence of other competing metal ions. Furthermore, confocal laser scanning microscopic experiments have shown that the sensor **1** can be used to detect Hg^{2+} in living cells. Consequently most excellent of our information, no sensors are available which can sense the cytoplasmic Hg^{2+} in the cancer cells and has huge potential application for diagnostic area.

References

1. J. P. Desvergne, A. W. Czarnik, *Chemosensors of Ion and Molecule Recognition*, Eds.: Kluwer Academic Publishers: Dordrecht, The Netherlands, 1997.
2. (a) A. P. de Silva, H. Q. N. Gunaratne, T. Gunnlaugsson, A. J. M. Huxley, C. P. McCoy, J. T. Rademacher, T. E. Rice, *Chem. Rev.* 1997, **97**, 1515; (b) A. P. de Silva, D. B. Fox, A. J. M. Huxley, T. S. Moody, *Coord. Chem. Rev.* 2000, **205**, 41.
3. (a) G. Orellana, M. C. Moreno-Bondi, *Frontiers in Chemical Sensors: Novel Principles and Techniques*, Springer: New York, **2005**; (b) E. V. Anslyn, *Angew Chem. Int. Ed. Engl.* 2001, **40**, 3119.
4. (a) B. Liu, F. Zeng, G. Wu, S. Wu, *Analyst*, 2012, **137**, 379 (b) C. McDonagh, C. S. Burke, B. D. MacCraith, *Chem. Rev.* 2008, **108**, 400. (c) H. N. Kim, W. X. Ren, J. S. Kim, J. Yoon, *Chem. Soc. Rev.*, 2012, **41**, 3210.
5. (a) R. Von Burg, *J. Appl. Toxicol.* **1995**, **15**, 483; (b) M. F. Wolfe, S. Schwarzbach, R. A. Sulaiman, *Environ. Toxicol. Chem.* 1998, **17**, 146. (c) Z. Yan, M. Yuen, L. Hu, P. Sun, C. Lee, *RSC Adv.*, 2014, **4**, 48373.
6. X. Zhang, Y. Xiao, X. Qian, *Angew. Chem., Int. Ed.* 2008, **47**, 8025.
7. A. Renzoni, F. Zino, E. Franchi, *Environ. Res., Sect. A*, 1998, **77**, 68.
8. A.T. Wright, E.V. Anslyn, *Chem. Soc. Rev.* 2006, **35**, 14.
9. (a) Y. Zhao, Z. Lin, C. He, H. Wu, and C. Duan, *Inorg. Chem.* 2006, **45**, 10013; (b) M. Taki, K. Akaoka, S. Iyoshi, and Y. Yamamoto, *Inorg. Chem.* 2012, **51**, 13075.
10. (a) P. Mahato, S. Saha, P. Das, H. Agarwalla, Amitava Das, *RSC Adv.*, 2014, **4**, 36140; (b) T. Zhang, G. She, X. Qi, L. Mu, *Tetrahedron*, 2013, **69**, 7102.
11. K. Tayade, B. Bondhopadhyay, A. Basu, G. Krishna Chaitanya, S. K. Sahoo, S. Attarde, N. Singh, A. Kuwar, *Talanta*, 2014, **122**, 16.

12. (a) M. Y. Chae, A. W. Czarnik, *J. Am. Chem. Soc.* 1992, **114**, 9704. (b) T. Anand, G. Sivaraman, A. Mahesh, D. Chellappa, *Anal. Chimica Acta*, 2015, **853**, 596. (c) G. Sivaraman, T. Anand, D. Chellappa, *Chem Plus Chem*, 2014, **79**, 1761.
13. S. Patil, U. Fegade, S. K. Sahoo, A. Singh, J. Marek, N. Singh, R. Bendre, A. Kuwar, *ChemPhysChem*, 2014, **15**, 2230.
14. H.A. Benesi, J.H. Hildebrand, *J. Am. Chem. Soc.* 1949, **71**, 2703.
15. (a) W. Liu, J. Chen, L. Xu, J. Wu, H. Xu, H. Zhang, P. Wang, *Spectrochim Acta A*, 2012, **85**, 38.; (b) T. Zhang, G. She, X. Qi, L. Mua, *Tetrahedron*, 2013, **69**, 7102; (c) R. Kavitha, T. Stalin, *Journal of Luminescence*, 2014, **149**, 12.
16. H. B. Schlegel, G. E. Scuseria, M. A. Robb, J. R. Cheeseman, G. Scalmani, V. Barone, B. Mennucci, G. A. Petersson, H. Nakatsuji, M. Caricato, X. Li, H. P. Hratchian, A. F. Izmaylov, J. Bloino, G. Zheng, J. L. Sonnenberg, M. Hada, M. Ehara, K. Toyota, R. Fukuda, J. Hasegawa, M. Ishida, T. Nakajima, Y. Honda, O. Kitao, H. Nakai, T. Vreven, J. A. Montgomery, Jr., J. E. Peralta, F. Ogliaro, M. Bearpark, J. J. Heyd, E. Brothers, K. N. Kudin, V. N. Staroverov, R. Kobayashi, J. Normand, K. Raghavachari, A. Rendell, J. C. Burant, S. S. Iyengar, J. Tomasi, M. Cossi, N. Rega, J. M. Millam, M. Klene, J. E. Knox, J. B. Cross, V. Bakken, C. Adamo, J. Jaramillo, R. Gomperts, R. E. Stratmann, O. Yazyev, A. J. Austin, R. Cammi, C. Pomelli, J. W. Ochterski, R. L. Martin, K. Morokuma, V. G. Zakrzewski, G. A. Voth, P. Salvador, J. J. Dannenberg, S. Dapprich, A. D. Daniels, Ö. Farkas, J. B. Foresman, J. V. Ortiz, J. Cioslowski and D. J. Fox, *Gaussian 09*, Revision A.1, Gaussian, Inc., Wallingford CT, 2009.
17. V. Bhalla, V. Vij, R. Tejpal, G. Singh, M. Kumar, *Dalton Trans.*, 2013, **42**, 4456.
18. J. Du, J. Fan, X. Peng, P. Sun, J. Wang, H. Li, S. Sun, *Org. Lett.*, 2010, **12**, 476.
19. M. Yang, C. R. Lohani, H. Cho, K. Lee, *Org. Biomol. Chem.*, 2011, **9**, 2350.
20. B. Liu, F. Zeng, G. Wu, S. Wu, *Analyst*, 2012, **137**, 3717

21. S. Madhu, R. Kalaiyarasi, S. K. Basu, S. Jadhav, M. Ravikanth, *J. Mater. Chem. C*, 2014, **2**, 2534.
22. B. P. Joshi, C. R. Lohani, K. Lee, *Org. Biomol. Chem.*, 2010, **8**, 3220.
23. J. Liu, M. Yua, X. Wang, Z. Zhang, *Spectrochim. Acta, Part A*, 2012, **93**, 245.
24. S. K. Kim, K. M. K. Swamy, S. Y. Chung, H. N. Kim, M. J. Kim, Y. Jeong and J. Yoon, *Tetrahedron Lett.*, 2010, **51**, 3286.
25. M. Vedamalai and S. P. Wu, *Org. Biomol. Chem.*, 2012, **10**, 5410.
26. G. Sivaraman, T. Anand, D. Chellappa, *RSC Adv.*, 2012, **2**, 10605.
27. T. Anand, G. Sivaraman, D. Chellappa, *Spectrochimica Acta Part A: Molecular and Biomolecular Spectroscopy*, 2014, **123**, 18.